

Hydration-dependent dynamic crossover phenomenon in protein hydration water

Zhe Wang,¹ Emiliano Fratini,² Mingda Li,¹ Peisi Le,¹ Eugene Mamontov,³ Piero Baglioni,² and Sow-Hsin Chen^{1,*}

¹*Department of Nuclear Science and Engineering, Massachusetts Institute of Technology, Cambridge, Massachusetts 02139, USA*

²*Department of Chemistry and CSGI, University of Florence, Sesto Fiorentino, Florence I-50019, Italy*

³*Spallation Neutron Source, Oak Ridge National Laboratory, Oak Ridge, Tennessee 37831, USA*

(Received 2 July 2014; published 8 October 2014)

The characteristic relaxation time τ of protein hydration water exhibits a strong hydration level h dependence. The dynamic crossover is observed when h is higher than the monolayer hydration level $h_c = 0.2\text{--}0.25$ and becomes more visible as h increases. When h is lower than h_c , τ only exhibits Arrhenius behavior in the measured temperature range. The activation energy of the Arrhenius behavior is insensitive to h , indicating a local-like motion. Moreover, the h dependence of the crossover temperature shows that the protein dynamic transition is not directly or solely induced by the dynamic crossover in the hydration water.

DOI: [10.1103/PhysRevE.90.042705](https://doi.org/10.1103/PhysRevE.90.042705)

PACS number(s): 87.15.H—, 64.70.pm, 87.16.—b

I. INTRODUCTION

Proteins are dynamic systems that strongly couple with their environment [1]. Experimental studies show that the protein hydration water plays a key role in many aspects of protein behavior, which include the mean square displacement of the protein constituent atoms [2–4], the subpicosecond collective vibrations [5–8], the intraprotein α and β fluctuations [9,10], and the protein enzymatic activity [11]. Thus the study of the protein hydration water is crucial for the understanding of protein dynamics. One observation of the protein hydration water is the so-called dynamic crossover [12], which is referred to as a transition in the characteristic relaxation time of the hydration water molecule from an Arrhenius behavior at low temperatures to a super-Arrhenius behavior at high temperatures. At ambient pressure, the dynamic crossover takes place at $T_X = 220$ K for hydrated lysozyme (with hydration level h equals 0.3, i.e., 0.3 g of water/g of protein). This phenomenon is of particular interest, partially because (i) the crossover temperature T_X of the hydration water is close to the transition temperature of the so-called protein dynamic transition (PDT) [13] T_D and thus it is conjectured that the PDT is induced by the dynamic crossover of the hydration water [12] and (ii) this crossover is interpreted as an anomalous feature of the structural relaxation of the hydration water and is ascribed to the existence of the high-density liquid and low-density liquid phases in the supercooled water [12]. To date, this phenomenon and its physical implications are still largely debated [14–19]. Doster *et al.* [17] state that the crossover observed in Ref. [12] is due to numerical errors in the data analysis protocol and can be ruled out with an improved analysis method. Magazù *et al.* [16] and Schirò *et al.* [19] draw opposite conclusions on the role that the dynamic crossover plays in the onset of the PDT with resolution-dependent neutron scattering experiments. Swenson *et al.* [14], Pawlus *et al.* [15], and Fenimore *et al.* [18] propose that the appearance of the dynamic crossover in the hydration water is due to the existences of two different relaxation processes, the structural relaxation and a secondary relaxation, rather than a qualitative

change from an Arrhenius behavior to a super-Arrhenius behavior of the structural relaxation time.

II. EXPERIMENT

In order to clarify some of the controversies over the dynamic crossover in the protein hydration water, we investigate the characteristic relaxation time of the hydration water of lysozyme at three hydration levels, $h = 0.18, 0.30$, and 0.45 , with quasielastic neutron scattering (QENS). The sample preparation can be found in the Appendix. The experiment was performed on the backscattering spectrometer BASIS [20] at the Spallation Neutron Source (SNS), Oak Ridge National Laboratory (ORNL). In this study, for each hydration level, the spectra at two Q values, 0.5 and 0.9 \AA^{-1} , were measured. The energy window for data analysis is from -20 to $20 \mu\text{eV}$ and the energy resolution of the spectrometer is $3.4 \mu\text{eV}$. For lysozyme, the hydration level of $0.2\text{--}0.25$ (denoted by h_c) is critical: The hydrogen-bonding sites on the protein surface are just completely saturated with water at this hydration level [11]. We stress that $h = 0.30$ and 0.45 , the two higher hydration levels studied, are well above h_c . In contrast, the lowest hydration level $h = 0.18$ is slightly lower than h_c .

III. RESULT AND DISCUSSION

The measured scattering intensity relevant to the water in equilibrium with the protein $I_{\text{H}_2\text{O}}(E)$ is obtained from the signal of the H_2O -hydrated sample $I_{\text{lys,H}_2\text{O}}(E)$ subtracted by the signal of the D_2O -hydrated sample $I_{\text{lys,D}_2\text{O}}(E)$ at the same hydration level. Thus the obtained spectra were fit with the equation

$$\begin{aligned} I_{\text{lys,H}_2\text{O}}(E) - I_{\text{lys,D}_2\text{O}}(E) \\ = I_{\text{H}_2\text{O}}(E) = \{p\delta(E) + (1-p)\mathcal{F}[F_s(t)]\} \otimes R(E) + B, \end{aligned} \quad (1)$$

where \mathcal{F} denotes a time Fourier transform, $R(E)$ is the energy resolution function, \otimes is the convolution operator, p is the elastic fraction, and B is a background constant. The elastic component contains the incoherent signal from the exchanged hydrogen atoms as well as the immobilized water molecules near charged groups. Here $F_s(t)$ is the self-intermediate

*Corresponding author: sowhsin@mit.edu

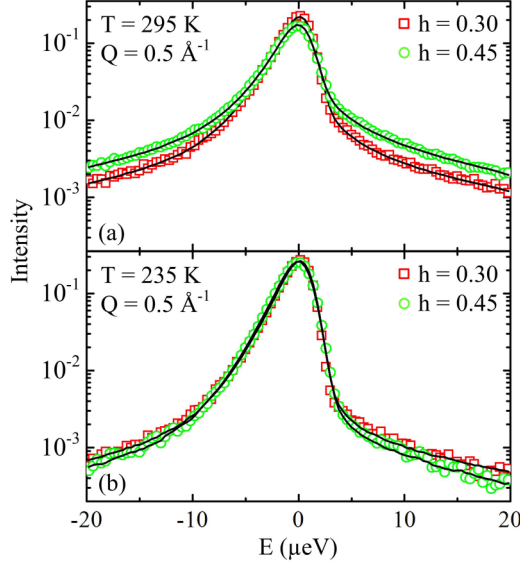


FIG. 1. (Color online) Quasielastic neutron scattering spectra of the hydration water at (a) $T = 295$ K and (b) 235 K for the sample with $h = 0.30$ (red open squares) and 0.45 (green open circles) at $Q = 0.5 \text{ \AA}^{-1}$. The fitted curves are denoted by solid lines. At 295 K, the protein hydration water at $h = 0.30$ is seen to relax more slowly than the one at $h = 0.45$. However, this ordering is reversed at 235 K.

scattering function (SISF). For supercooled water, the decay of $F_s(t)$ has two steps [21]. The first step corresponds to some localized motion on a subpicosecond time scale. This motion is beyond the dynamic range of the spectrometer. The second step (long time) is highly nonexponential and is usually described by a stretched exponential decay form [21]. To account for these considerations, the experimental SISF is modeled with the equation

$$F_s(t) \approx A(Q)\exp[-(t/\tau)^\beta], \quad (2)$$

where $A(Q)$ is the amplitude after the initial step, τ is the characteristic relaxation time of the long-time relaxation, and β is the stretching exponent. The mean characteristic relaxation time $\langle\tau\rangle$ is calculated from τ and β by $\langle\tau\rangle = \beta^{-1}\Gamma(\beta^{-1})\tau$. In this study, β is fixed to 0.5, just as in the analysis of Doster *et al.* [17] and a previous work by our group [12]. In addition, we have taken the elastic fraction p to be of the form $p(Q) = p_0A(Q)$, with p_0 constant. This is because both $p(Q)$ and $A(Q)$ are expected to have the form of a Debye-Waller factor. For each sample and a specific Q , the value of p_0 was obtained from the fit of the spectrum at 295 K since the elastic fraction $p(Q)$ is most easily distinguished at the highest temperature. The analysis method introduced here has been successfully applied to study the single-particle dynamics of the deeply cooled water confined in silica matrices [22]. Figure 1 shows selected measured spectra for the samples with $h = 0.30$ and 0.45 along with the corresponding calculated curves fitted by Eq. (1). In principle, this method is the same as the one Doster *et al.* used in Ref. [17], in which the authors highlight that no crossover is observed in the hydration water of protein in the QENS experiment. Moreover, when calculating the term $\mathcal{F}[F_s(t)]$ [denoted by $S_{\text{th}}(Q, E)$], we use a very small interval

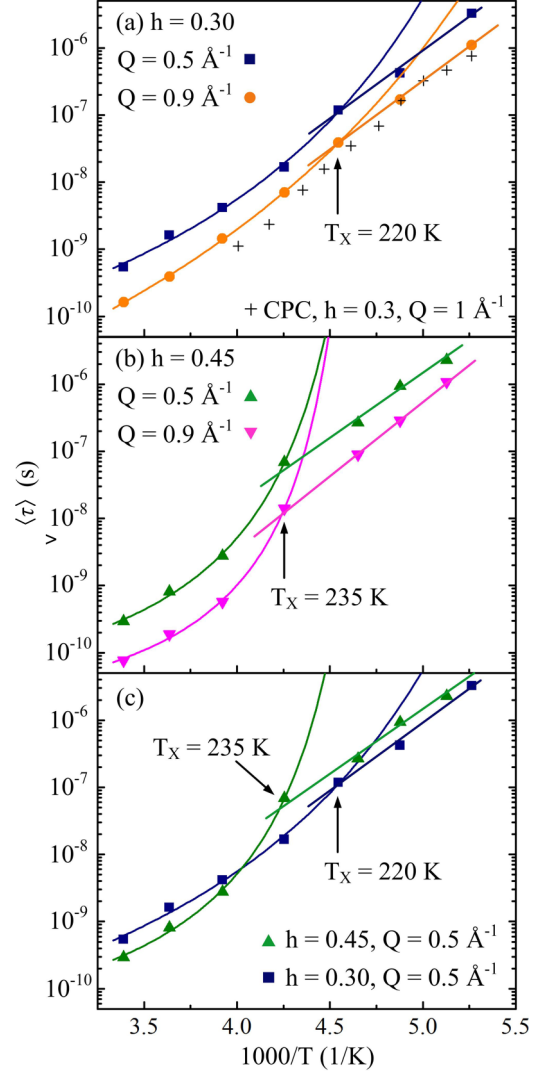


FIG. 2. (Color online) Arrhenius plot of the mean characteristic relaxation time $\langle\tau\rangle$ for the samples with $h = 0.30$ and 0.45 at (a) $Q = 0.5$ (blue squares) and 0.9 \AA^{-1} (orange circles) for the sample with $h = 0.30$ and (b) $Q = 0.5$ (green up triangles) and 0.9 \AA^{-1} (magenta down triangles) for the samples with $h = 0.45$. The dynamic crossover takes place at about 220 K in the former case and at about 235 K in the latter case. The result of Doster *et al.* [17] for the CPC with $h = 0.3$ and at $Q = 1 \text{ \AA}^{-1}$ is also plotted in (a) and is denoted by + markers. (c) shows the $\langle\tau\rangle$ at $Q = 0.5 \text{ \AA}^{-1}$ for both cases of $h = 0.30$ and 0.45. It is seen that the hydration water at $h = 0.45$ exhibits a more visible dynamic crossover than that at $h = 0.30$.

in the sequence of E to guarantee that the Riemann sum of the normalized $S_{\text{th}}(Q, E)$ converges to 1; thus the numerical problem pointed out by Doster *et al.* in Ref. [17] will not appear. Therefore, a direct comparison between the results in this study and in Ref. [17] could be performed.

Figure 2(a) shows the $\langle\tau\rangle$ for the sample with $h = 0.30$. The higher-temperature data exhibit super-Arrhenius behavior, which can be fit by the Vogel-Fulcher-Tammann (VFT) relation $\langle\tau\rangle = \tau_0\exp[DT_0/(T - T_0)]$. The lower-temperature data exhibit Arrhenius behavior, which can be fit by the Arrhenius relation $\langle\tau\rangle = \tau_0\exp(E_a/k_B T)$. In this case, the

TABLE I. Parameters in the VFT relation and the Arrhenius relation for $h = 0.30$ and 0.45 .

h	Q (\AA^{-1})	D	T_0 (K)	E_a (kcal/mol)
0.30	0.5	4.96	148	9.20
0.30	0.9	9.98	123	9.26
0.45	0.5	1.41	201	8.93
0.45	0.9	1.03	207	9.85

crossing temperature of these two fits, i.e., the dynamic crossover temperature T_X , is 220 K for all the measured Q values. As h increases to 0.45, the dynamic crossover shifts to 235 K, as shown in Fig. 2(b). The parameters D , T_0 , and E_a for these two samples are listed in Table I. It can be seen that the parameters for the higher-temperature data D and T_0 have a strong h dependence. This leads to a significant difference in the curvature of the $\langle \tau \rangle$ in the Arrhenius plot at higher temperatures as h increases from 0.30 to 0.45, as shown in Fig. 2(c). Such a difference that the T dependence of $\langle \tau \rangle$ with $h = 0.45$ exhibits a stronger super-Arrhenius feature than that with $h = 0.30$ is also reflected in the measured spectra. As shown in Fig. 1, at $T = 295$ K, the hydration water at $h = 0.45$ relaxes faster than that at $h = 0.30$, indicated by a stronger inelastic scattering in the spectrum; however, as the temperature decreases to 235 K, this ordering is reversed: The hydration water at $h = 0.45$ relaxes slower than that at $h = 0.30$, indicated by a weaker inelastic scattering in the spectrum. For the samples with $h = 0.30$ and 0.45 , the hydration level is well above the monolayer hydration level h_c , thus the hydration water molecules are abundant enough to form an open tetrahedral structure. Under these circumstances, a molecule is likely to be trapped in a cage consisting of its neighboring molecules. The translational diffusion jump of this molecule requires cage breaking that is associated with simultaneous breaking of several hydrogen bonds. As T decreases, the local order surrounding a molecule is enhanced, which leads to a significant increase of the structural relaxation time [21]. Subsequently, this collective relaxation process exhibits a non-Arrhenius T dependence. As h increases, the cage effect is enhanced, which causes the T dependence of $\langle \tau \rangle$ to deviate from the Arrhenius behavior more significantly. In contrast to D and T_0 , the activation energy E_a for the lower-temperature data is insensitive to h , as shown in Table I. In addition, we plot the neutron scattering result for the hydration water of deuterated C-phycoerythrin (CPC) with $h = 0.3$ and at $Q = 1 \text{ \AA}^{-1}$ in Fig. 2(a) [17]. Not surprisingly, the data agree well with our data for the sample with $h = 0.30$ and at $Q = 0.9 \text{ \AA}^{-1}$, due to the similar h , Q , and analysis method in these two cases. With the result of CPC, Doster *et al.* [17] conclude that no dynamic crossover happens. However, our analysis confirms that the dynamic crossover takes place when the hydration water is sufficient and it becomes more visible as h increases, due to the strong h dependence of the higher-temperature data. In fact, a similar phenomenon is also observed in the water confined in nanoporous silica material MCM-41. Faraone *et al.* [23] show that as the diameter of the confining pore increases from 14 to 18 \AA (thus the water content also increases), D changes from 4.62 to 1.47 and T_0

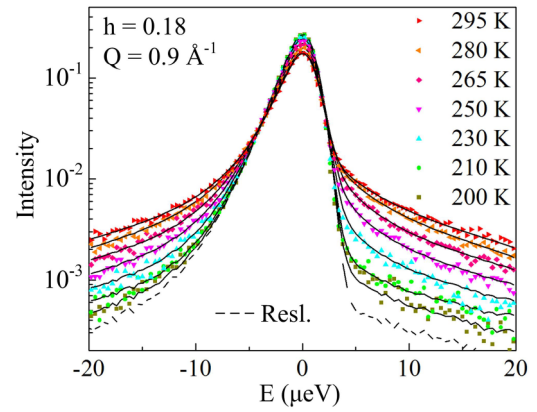


FIG. 3. (Color online) Quasielastic neutron scattering spectra of the hydration water along with the corresponding fitted curves (denoted by solid curves) at $h = 0.18$ and $Q = 0.9 \text{ \AA}^{-1}$. The energy resolution function is denoted by a dashed line.

changes from 170 to 200 K. Such h dependences of D and T_0 exhibit a similarity to the results of the protein hydration water shown in Table I. As a result, the T_X of the water confined in MCM-41 increases from 222 to 225 K as the size of the confining pore increases, which exhibits the same trend as in the case of the protein hydration water.

The spectra at $Q = 0.9 \text{ \AA}^{-1}$ for the hydration water at $h = 0.18$ are shown in Fig. 3 and the Arrhenius plot of the $\langle \tau \rangle$ is shown in Fig. 4. In this case, no significant crossover is observed and the T dependence of $\langle \tau \rangle$ can be well described by the Arrhenius relation in the measured temperature range. The activation energies E_a at $Q = 0.5$ and 0.9 \AA^{-1} , obtained from the fit with the Arrhenius relation, are 9.31 and 10.14 kcal/mol, respectively. As mentioned before, the hydration water of this sample merely saturates most of the polar groups on the protein surface. The chance to form an open tetrahedral structure is little. Therefore, it is likely that the water-surface interaction, rather than the water-water interaction, dominates the relaxation process. In fact, the disappearances of the

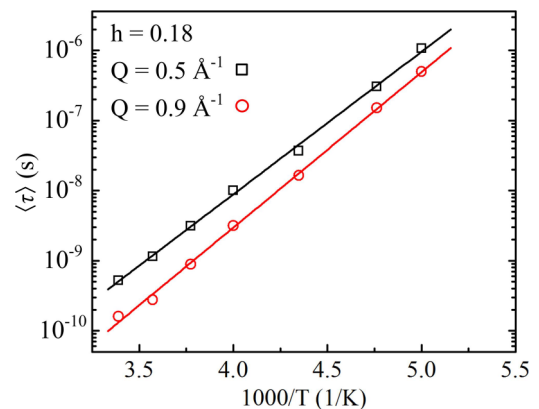


FIG. 4. (Color online) Arrhenius plot of the mean characteristic relaxation time $\langle \tau \rangle$ at $Q = 0.5$ (black open squares) and 0.9 \AA^{-1} (red open circles) for the sample with $h = 0.18$. In this case, the T dependence of $\langle \tau \rangle$ can be described by the Arrhenius relation in the measured temperature range.

super-Arrhenius behavior at higher temperatures and the dynamic crossover are also found in the hydration water of inorganic materials at low hydration levels [22,24,25]. Interestingly, the activation energies for this sample are similar to those for the lower-temperature data of the samples with $h = 0.30$ and 0.45 . Moreover, the activation energies obtained here, which are around 9–10 kcal/mol, agree well with the activation energies of the hydration water for many other soft and biological materials at low hydration levels [26]. The weak hydration level and environmental dependences of E_a suggest that the corresponding motions are local-like [26].

Owing to the similarity of T_X and T_D for the protein with $h = 0.3$, in a previous work [12], the authors tentatively ascribed the onset of the PDT to the dynamic crossover of the protein hydration water. This conjecture is under debate [16,19,27,28]. It is well known that most of proteins only function with sufficient hydration water. Therefore, to learn how proteins work, it is important to clarify the relation between the PDT and the dynamic crossover in hydration water. Roh *et al.* investigated the PDT of lysozyme at $h = 0.18$, 0.30 , and 0.45 (see Fig. 2 in Ref. [3]). Thus a direct comparison between the PDT and the dynamic crossover in protein hydration water can be performed. The common features of the PDT and the dynamic crossover can be summarized as follows: (i) Both of these phenomena appear at $h = 0.30$ and 0.45 and are strongly suppressed at $h = 0.18$ and (ii) both of them are enhanced as h increases. However, the h dependences of T_D and T_X are not similar to each other. According to Roh *et al.* [3], the values of T_D at $h = 0.30$ and 0.45 are both around 200 K, which is substantially different from the results of T_X shown in this study. Moreover, Paciaroni *et al.* [2] report that T_D even decreases as h increases. To account for these results, we conclude that the PDT is not directly or solely induced by the dynamic crossover in the protein hydration water.

IV. CONCLUSION

In summary, we investigated the single-particle dynamics of the protein hydration water at different hydration levels. The dynamic crossover phenomenon appears when h is higher than the monolayer hydration level $h_c = 0.2$ – 0.25 and becomes more visible as h increases in the measured range. It disappears when h is slightly lower than h_c and in this case τ only exhibits Arrhenius behavior in the whole range of measured temperature. The higher-temperature data for the samples with $h = 0.30$ and 0.45 , which exhibit a super-Arrhenius behavior, are sensitive to h . In contrast, the lower-temperature data,

which exhibit Arrhenius behavior, are relatively insensitive to h and display local-like characteristics. These results highlight the importance of the tetrahedral hydrogen-bond structure in the dynamics of the hydration water. In addition, the crossover temperature exhibits a different h dependence from that of the PDT temperature. This difference clearly shows that the PDT is not directly or solely induced by the dynamic crossover in the hydration water.

ACKNOWLEDGMENTS

The research at MIT was supported by a grant from the Office of Basic Energy Sciences, US Department of Energy under Contract No. DE-FG02-90ER45429. The neutron scattering experiments at SNS, ORNL were supported by the Scientific User Facilities Division, Office of Basic Energy Sciences, US Department of Energy. E.F. and P.B. acknowledge financial support from Consorzio per lo Sviluppo dei Sistemi a Grande Interfase (CSGI). Z.W. thanks Prof. X.-Q. Chu and Dr. C. E. Bertrand for their valuable advices.

APPENDIX: SAMPLE PREPARATION

In this study, six hydrated lysozyme samples were prepared: samples hydrated with H_2O at $h = 0.18$, 0.30 , and 0.45 , and samples hydrated with D_2O at $h = 0.20$, 0.33 , and 0.49 . The scattering signal relevant only to water in equilibrium with protein is obtained from the signal of the H_2O -hydrated sample subtracted by the signal of the D_2O -hydrated sample at the sample hydration level. Three times crystallized, dialyzed, and lyophilized hen egg white lysozyme (L7651) was purchased from Sigma-Aldrich (Milan). The protein powder was extensively lyophilized to remove any remaining water. In the case of D_2O -hydrated samples, a batch of lysozyme was first dissolved in pure D_2O at a concentration of 6 mM and then stirred at $4^\circ C$ for 48–72 h. After removing aggregates by filtration (cutoff 200 nm), the protein solution was extensively lyophilized. These steps were repeated three times to exchange all the labile hydrogen atoms. The H_2O - (or D_2O -) hydrated powders were obtained by isopiesticly exposing the as-received lyophilized lysozyme (or D-exchanged lysozyme) to H_2O (or D_2O) vapor in a closed chamber at $4^\circ C$. The water content of the samples was followed by weighing and confirmed by thermogravimetric analysis in the $25^\circ C$ – $140^\circ C$ range. Final hydration levels resulted in $h = 0.18, 0.30, 0.45$ and $h = 0.19, 0.33, 0.49$ for the H_2O - and D_2O -hydrated samples, respectively.

-
- [1] H. Frauenfelder, G. Chen, J. Berendzen, P. W. Fenimore, H. Jansson, B. H. McMahon, I. R. Stroe, J. Swenson, and R. D. Young, *Proc. Natl. Acad. Sci. USA* **106**, 5129 (2009).
- [2] A. Paciaroni, S. Cinelli, and G. Onori, *Biophys. J.* **83**, 1157 (2002).
- [3] J. H. Roh, J. E. Curtis, S. Azzam, V. N. Novikov, I. Peral, Z. Chowdhuri, R. B. Gregory, and A. P. Sokolov, *Biophys. J.* **91**, 2573 (2006).
- [4] G. Schirò, C. Caronna, F. Natali, M. Koza, and A. Cupane, *J. Phys. Chem. Lett.* **2**, 2275 (2011).
- [5] A. Orecchini, A. Paciaorni, A. R. Bizzarri, and S. Cannistraro, *J. Phys. Chem. B* **105**, 12150 (2001).
- [6] A. Orecchini, A. Paciaroni, A. De Francesco, C. Petrillo, and F. Sacchetti, *J. Am. Chem. Soc.* **131**, 4664 (2009).
- [7] Z. Wang, C. E. Bertrand, W.-S. Chiang, E. Fratini, P. Baglioni, A. Alatas, E. Alp, and S.-H. Chen, *J. Phys. Chem. B* **117**, 1186 (2013).

- [8] Z. Wang, W.-S. Chiang, P. Le, E. Fratini, M. Li, A. Alatas, P. Baglioni, and S.-H. Chen, *Soft Matter* **10**, 4298 (2014).
- [9] P. W. Fenimore, H. Frauenfelder, B. H. McMahon, and F. G. Parak, *Proc. Natl. Acad. Sci. USA* **99**, 16047 (2002).
- [10] P. W. Fenimore, H. Frauenfelder, B. H. McMahon, and R. D. Young, *Proc. Natl. Acad. Sci. USA* **101**, 14408 (2004).
- [11] G. Careri, E. Gratton, P.-H. Yang, and J. A. Rupley, *Nature (London)* **284**, 572 (1980).
- [12] S.-H. Chen, L. Liu, E. Fratini, P. Baglioni, A. Faraone, and E. Mamontov, *Proc. Natl. Acad. Sci. USA* **103**, 9012 (2006).
- [13] W. Doster, S. Cusack, and W. Petry, *Nature (London)* **337**, 754 (1989).
- [14] J. Swenson, H. Jansson, and R. Bergman, *Phys. Rev. Lett.* **96**, 247802 (2006).
- [15] S. Pawlus, S. Khodadadi, and A. P. Sokolov, *Phys. Rev. Lett.* **100**, 108103 (2008).
- [16] S. Magazù, F. Migliardo, and A. Benedetto, *J. Phys. Chem. B* **115**, 7736 (2011).
- [17] W. Doster, S. Busch, A. M. Gaspar, M.-S. Appavou, J. Wuttke, and H. Scheer, *Phys. Rev. Lett.* **104**, 098101 (2010).
- [18] P. W. Fenimore, H. Frauenfelder, S. Magazù, B. H. McMahon, F. Mezei, F. Migliardo, R. D. Young, and I. Stroe, *Chem. Phys.* **424**, 2 (2013).
- [19] G. Schirò, F. Natali, and A. Cupane, *Phys. Rev. Lett.* **109**, 128102 (2012).
- [20] E. Mamontov and K. W. Herwig, *Rev. Sci. Instrum.* **82**, 085109 (2011).
- [21] S.-H. Chen, C. Liao, F. Sciortino, P. Gallo, and P. Tartaglia, *Phys. Rev. E* **59**, 6708 (1999).
- [22] C. E. Bertrand, K.-H. Liu, E. Mamontov, and S.-H. Chen, *Phys. Rev. E* **87**, 042312 (2013).
- [23] A. Faraone, L. Liu, C.-Y. Mou, C.-W. Yen, and S.-H. Chen, *J. Chem. Phys.* **121**, 10843 (2004).
- [24] E. Mamontov, H. O'Neill, Q. Zhang, W. Wang, and D. J. Wesolowski, *J. Phys. Condens. Matter* **24**, 064104 (2012).
- [25] E. Mamontov, L. Vlcek, D. J. Wesolowski, P. T. Cummings, J. Rosenqvist, W. Wang, D. R. Cole, L.M. Anovitz, and G. Gasparovic, *Phys. Rev. E* **79**, 051504 (2009).
- [26] S. Cerveny, G. A. Schwartz, R. Bergman, and J. Swenson, *Phys. Rev. Lett.* **93**, 245702 (2004).
- [27] E. Mamontov and X.-Q. Chu, *Phys. Chem. Chem. Phys.* **14**, 11573 (2012).
- [28] X.-Q. Chu, A. Faraone, C. Kim, E. Fratini, P. Baglioni, J. B. Leao, and S.-H. Chen, *J. Phys. Chem. B* **113**, 5001 (2009).